World Journal of Nuclear Science and Technology, 2016, 6, 23-42
Published Online January 2016 in SciRes. http://www.scirp.org/journal/wjnst
http://dx.doi.org/10.4236/wjnst.2016.61003

Thermal Stress in HFEF Hot Cell Windows Due to an In-Cell Metal Fire

Charles W. Solbrig*, Stephen A. Warmann

Idaho National Laboratory, Idaho Falls, USA
Email: *Charles.solbrig@inl.gov, Stephen.warmann@inl.gov

Received 16 July 2015; accepted 3 January 2016; published 6 January 2016

Abstract

This work investigates an accident during the pyrochemical extraction of Uranium and Plutonium from PWR spent fuel in an argon atmosphere hot cell. In the accident, the heavy metals (U and Pu) being extracted are accidently exposed to air from a leaky instrument penetration which goes through the cell walls. The extracted pin size pieces of U and Pu metal readily burn when exposed to air. Technicians perform the electrochemical extraction using manipulators through a 4 foot thick hot cell concrete wall which protects them from the radioactivity of the spent fuel. Four foot thick windows placed in the wall allow the technicians to visually control the manipulators. These windows would be exposed to the heat of the metal fire. This analysis determines if the thermal stress caused by the fire would crack the windows and if the heat would degrade the window seals allowing radioactivity to escape from the cell.

Keywords

Pyrophoric Metals, Thermal Stress, Nuclear Fuel Reprocessing, Hot Cells, Brittle Materials, Yield Stress

1. Introduction

This is the first time the complete process of reprocessing PWR fuel to produce fuel for use in Fast Reactors will be demonstrated on a lab scale. This project has introduced a new safety concern in the Hot Fuel Examination Facility hot cell. The concern is the heat generated by the accidental burning of the heavy metals (U and Pu) being extracted when accidently exposed to air from a leaky instrument or manipulator penetration which goes through the cell walls. The extracted pin size pieces of U and Pu metal readily burn when exposed to air. Technicians perform the electrochemical extraction using manipulators through a 4 foot thick hot cell concrete wall which

*Corresponding author.

How to cite this paper: Solbrig, C.W. and Warmann, S.A. (2016) Thermal Stress in HFEF Hot Cell Windows Due to an In-Cell Metal Fire. *World Journal of Nuclear Science and Technology*, **6**, 23-42. http://dx.doi.org/10.4236/wjnst.2016.61003

protects them from the radioactivity of the spent fuel. Four foot thick windows placed in the wall allow the technicians to visually control the manipulators. These windows would be exposed to the heat of the metal fire. This analysis determines if the thermal stress caused by the fire would crack the windows and if the heat would degrade the window seals allowing radioactivity to escape from the cell and the oil reservoir which makes up part of the window would leak into the cell to add to the fire.

The heat transmitted to a window from burning heavy metal (HM) depends on the heat generated and the location of the material relative to the window. The window components and surrounding concrete are analyzed with a two-dimensional (depth and width of window) heat transfer model and a thermal stress model. The heat reaching the window from the fire is applied uniformly or with a distribution over the window surface. The distribution represents the thermal radiation view factor due to materials of different shapes.

The window can only receive heat from one side of the fire the maximum exposures 25% of the heat released. All this heat is applied directly to the window or the window and concrete (which does not account for heat loss to the cell gas by convection).

A thermal stress model is used to determine if the stress in any of the glass panes which make up the window exceeds the glass tensile stress strength which would cause cracking. The maximum amount of exposed HM (12 kg) was used as the heat source. The heat source was assumed to be comprised of dendrites that release a constant power until all the metal is reacted, which occurs in 31.8 minutes. The exposed metal may be in open canisters. A cylindrical geometry is assumed to result in a sine wave distribution of heat flux on the window. The cold side of a window pane will develop the tensile stress due to expansion of the hot side and therefore, is the side prone to cracking. The highest stress is on the cold side surface.

More concentrated HM in the form of a puck or button has much less surface area per unit volume than dendrites making the heat source density less than that of the dendrites (A denser heat source also has a higher ignition temperature and is less likely to burn.). A concentration of the heat flux was used to determine how much more stress HM burning in acylindrical container would provide than a uniform source. The seals are made of polyvinyl chloride (PVC) and can decompose (140˚C) and melt at lower temperatures (160˚C) compared to the other window components of concrete, metal, and glass. Thus, in some cases, the heat-flux term will be applied and concentrated near the window edge.

A previous study [1] developed for the facility safety analysis report [2] investigated the effect on the cell of exposing 62 kg of dendrites during a cell boundary breakage event. This amount generates 150 kW of power. The increased cell average wall temperatures (15˚C increase) and cell atmosphere temperatures (35˚C increase) were not enough to vaporize or decompose any material. There is no concern with a cell flashover to occur with the 150 kW heat release. For burning to occur (cell flashover), it is necessary to increase cell temperature enough to release gases from cell flammable material. The heat release from this incident 12 kg ∗ 150 kW/62 kg = 30 kW is less and would have less effect upon the cell than those considered in ECAR-534.

Radiant heat received on the glass surface on the interior of the cell is transmitted through the glass and concrete by conduction only. Although the glass window has a visible transmissivity of 38% to visible light, the majority of the heat produced will be in the infrared. In the infrared region (*i.e.*, wavelengths greater than 0.8 micron), glass is opaque for wavelengths greater than 5 microns but transmits some radiation (perhaps 38%) for wave lengths from 0.8 to 5 microns. So some is transferred through the glass by radiation and some by conduction. This model assumes all the heat is passed by conduction. This assumption increases the temperature gradients in the glass and the thermal stress and is and so the model is very conservative. Heat loss back to the cell from the window is conservatively neglected. Combustion of the metal is assumed to be a constant rate until the metal is consumed. Reduction in the rate from oxide buildup could produce lower temperatures and stress.

2. Method

Equation (1) gives the conduction equation for the temperature T in two dimensions in region i as:

$$\rho_i C_{pi} \frac{\partial T_i}{\partial t} = k_i \frac{\partial^2 T_i}{\partial x^2} + k_i \frac{\partial^2 T_i}{\partial y^2} + q_i \tag{1}$$

where

ρ = density,

C_p = specific heat,

k = thermal conductivity,
q = heat generation rate per unit volume,
t = time,
x = horizontal axis,
y = vertical axis,
i = region or material.

The interface condition equating heat fluxes between two regions i and j is shown in Equation (2).

$$k_i \frac{\partial T_i}{\partial n} = k_j \frac{\partial T_j}{\partial n} \tag{2}$$

where
$n = x$ or y direction.

Equation (3) gives the boundary condition on the corridor side of the window is given as:

$$k_s \frac{\partial T}{\partial x} = h_c \left(T - T_c \right) \tag{3}$$

where
k_s = thermal conductivity of Pane G,
h_c = heat transfer coefficient of the corridor air and a function of the forced circulation of the cooling system,
T_c = temperature of the corridor.

The temperature derivative is evaluated on the right-hand side of the boundary. The building air circulation system is assumed to provide adequate flow around the outside of the cell to yield a high-heat transfer coefficient estimated at 100 W/m^2·K. The value of 100 was chosen for a previous study inside the ZPPR vault which has a high wind velocity so the heat transfer coefficient is high. However, since the temperature increase never went further from the cell side than the B pane, the heat transfer coefficient on the corridor side is irrelevant and the same results would have been obtained with a zero or a value 10 times as high since no heat is transferred at that surface.

Equation (4) shows the two boundaries on the right and left of the window are treated as insulated as well the cell side of the concrete and steel not exposed to the heat flux.

$$\frac{\partial T}{\partial y} = 0 \tag{4}$$

where y is the direction parallel to the cell wall.

In addition, the cell side of the window and concrete has a heat flux specified in Equation (5).

$$\frac{\partial T}{\partial n} = q \tag{5}$$

Equation (6) represents transverse thermal stress in a slab with a temperature distribution in the depth of the material. It is given in [3] and [4] as

$$\sigma_i = \frac{E\alpha}{1-\mu}\left(T_{avg} - T_i \right) \tag{6}$$

where
T_{avg} = average T in direction of the depth,
σ_i = stress at depth x_i,
E = Young's Modulus,
α = coefficient of thermal expansion,
μ = *Poisson's ratio*.

The thermal stress is calculated with a coefficient of thermal expansion in the glass of CTE = 9×10^{-6}/K, Young's modulus $E = 6.89 \times 10^4$ MPa = 10×10^6 psi; and Poisson's ratio, $\mu = 0.16$.Substituting the above values into Equation (6) gives the coefficient

$$\frac{E\alpha}{1-\mu} = 115.3846 \frac{\text{psi}}{K} \tag{7}$$

The tensile stress limit for glass is listed as 40 MPa = 5714 psi [5] and [6]. Toughened glass limit is three to five times greater than the tension stress limit at 120 to 200 MPa. The minimum value of the tensile stress limit reported in the literature appears to be the 5714 psi so to be conservative this limit will be used to evalulate possible damage to the glass. The same limit is applied to all panes of glass in the window.

The compression limit is 1000 MPa = 142,900 psi. Compression of glass is usually not a problem and none of the cases investigated in this study exhibit significant compression stress.

Figure 1 shows the equipment which will be operated in the hot cell in front of the 11 and 12 windows. It is a demonstration kilogram-scale integrated pyrochemical process. It will provide an evaluation of the recycling of used LWR oxide fuels via electrochemical technologies and a fast reactor. This evaluation of electrochemical recycling will focus on the improvement of process knowledge such that the technology's benefits to an overall fuel cycle can be better quantified. It will provide material balance data, evaluate process flow sheet options, and serve as a test bed for demonstration of safeguards and security technologies. It also includes the fabrication of several metal fuel rodlets, their irradiation in the Advanced Test Reactor, and post-irradiation examination (PIE) in HFEF.

The cell perimeter shielding windows are layered glass and optical oil (mineral oil) and provide shielding approximately equal to that of the walls. Each window is composed of lead glass slabs with thin layers of oil between them, plus a protective glass plates on the cell side and the corridor side. The cell side protective plate is supported by a frame hinged from the cell liner so that it can be swung into the cell for cleaning or replacement with the remote handling equipment.

Type A-1 windows (from Schott Optical Glass, Co.) are located at the main and deconcell window positions 1M, 2M, 4M, 5M, 7M, 9M, 11M, 13M, 15M, and 3D (see **Figure 2**). Each consists of six slabs of glass, labeled A through F. A type A-1 window consists of a steel-tank assembly inserted from the cold side that is bolted to the out-of-cell side of the window-liner flange. The tank has a primary gas seal bolted to its hot face to mate with the liner flange. The tank assembly contains three heavy glass slabs, labeled C and D (cerium-stabilized), and E. A type A-1 window has a hinged protection plate (A) and is equipped with a secondary-seal assembly at the in-cell end. The hot end is sealed with a 9-in.-thick slab of cerium-stabilized glass (B) and the cold end is sealed with a 20-mm-thick plate of the same type of glass (F) but with no cerium (total glass weight is 6734 lb). The remaining free space is filled with approximately 55 gal of clear mineral oil.

Overall light transmission is 38% (including the hinged protection plate). Total thickness of the glass is 48 in. (the window affords 149 density-in. Density inches = [specific gravity] × [thickness in inches of shielding]). The clear aperture is 24-in.-high and 40-in.-wide.

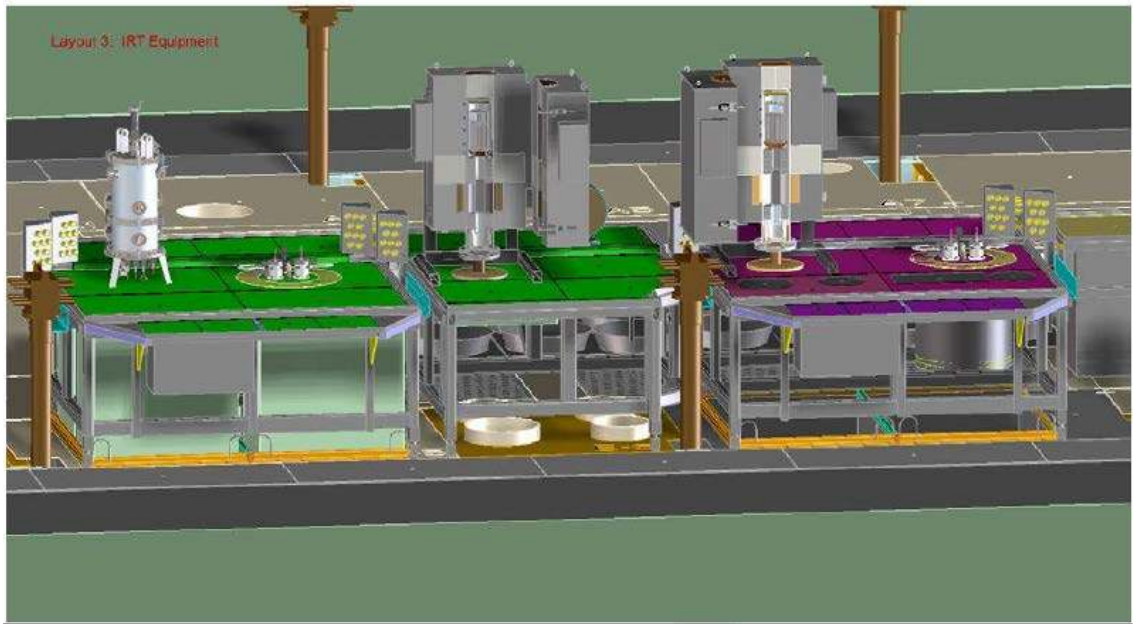

Figure 1. Equipment layout for HFEF Windows 11M and 12M.

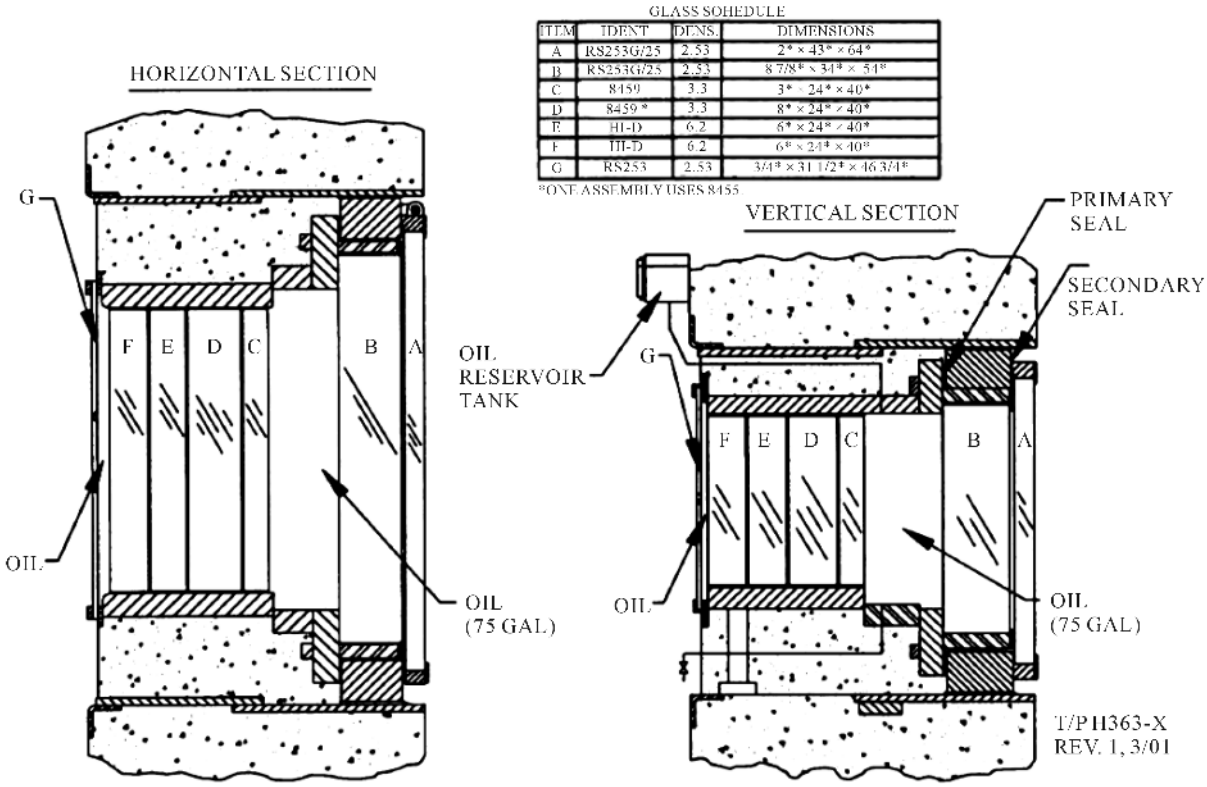

Figure 2. Type A-2 (Nuclear Pacific) radiation shielding window.

Drilled passageways in the liner flange are connected to a gas manifold that maintains an argongas pressure of 10-in.-wg. The primary and secondary seals (double seals with a center annulus) are made of extruded polyvinyl chloride. The center annulus is purged with argon gas in the primary seal and may be purged in the secondary seal if necessary. The center annulus is fed by the gas manifold.

The tank unit is supported near the cold end to prevent cantilevering the weight of the tank from the window-liner flange where the tank is bolted. During installation, a machine-leveling jack was placed under the support leg and adjusted to carry half the load. After installation and leak-checking the seals, the remaining annular space between the tank and window liner was carefully filled with a low-strength concrete grout with a specific gravity of 3.5 wg.

The oil reservoir (mounted on the operating corridor wall above the window) has a sight gauge with a capacity of about 1.6 gal of oil. Argon gas (at a pressure of 10-in.-wg) is piped into the free-air space in the top of the reservoir to prevent air from coming in contact with the window oil.

Type A-2 windows (from Nuclear Pacific, Inc.) are located at main and deconcell window positions 3M, 6M, 8M, 10M, 12M, 14M, 4D, and 5D. Each type A-2 window consists of seven slabs of glass, labeled A through G (see **Figure 2**). The Type A-2 window has been analyzed in this work but the results obtained apply to the Type A-1 window as well.

Viewing angles, shielding, primary and secondary seals, the oil reservoir, and grouting technique are the same for the type A-1 and A-2 windows. Tank structure is different (except for the flange at the hot end, which has to mate with existing window-liner flanges). The A-2 tank assembly contains four panes of glass (C, D, E, and F). The hot end of the tank is sealed with an 8-7/8-in.-thick slab of cerium-stabilized glass and the cold end is sealed with a 20-mm thickness of the same type of glass with no cerium. Total glass weight is 5933 lb. The remaining free space is filled with approximately 75 gal of clear mineral oil. Overall light transmission is approximately 38% (including the hinged protection plate, which is identical to that for a type A-1 window). The clear aperture is 24-in.-high and 40-in.-wide.A typical A-2 window is shown in **Figure 2**.

A typical window assembly is 64-in.-wide by 44-in.-high on the cell side, including the protective plate that tapers to 40-in.-wide by 24-in.-high on the corridor side.

Argon is contained between Panes A and B. Under cell pressure, no differential in pressure occurs from behind Pane A. Therefore, the cell pressure would not be applied to push the window out if a crack occurs.

75 gal of mineral oil is contained between PanB (8-7/8-in.-thick) and Pane C (3-in.-thick) with an estimated thickness of 11.625 in. A thin layer of oil is also between the remaining panes and maintained with an argon cover gas at a pressure of 10-in.-wg.There is concern that if the oil temperature increases then thermal expansion of the oil due to heating in the incident will cause an increase of pressure that cannot be relieved by the pressure system. This effect has been investigated in this study. The maximum oil temperature occurs in scenarios 6 where the average increase is 0.03 C resulting in an increase of 0.0014 gallons of the original 75 gallons and is therefore not of concern. (Note, this temperature increase is obtained in the highest temperature case which is investigated later in the paper. This temperature rise is discussed later preceding **Figure 23**).

The dimensions of type A-2 window components are included in **Table 1**.

A horizontal cut through the centerline of the window is modeled in the analysis. A vertical cross-section model would produce similar results. The information input to the computer code is summarized in **Figure 3**. Note this figure is not to scale. For example, Panes C through F are all 24-in.-wide and only represented by a single box. The number of increments used in the solution is noted and each of those panes are subdivided into 8 increments (length) and 5 (width), which is 40 subareas. The material specifications are shown in **Figure 4**.

The material properties used corresponding these numbers are listed below.

m = 1: cp(m) = 0.24 ∗ 4200: k(m) = 0.02 ∗ 1: rho(m) = 0.001: A(m) = “Arg Nu=1” 'J/kg C, W/m K, gm/cc

m = 2: cp(m) = 880: k(m) = 1.1: rho(m) = 2.1: A(m) = “kconcrete” ' J/kg C, W/m K, gm/cc”

m = 3: cp(m) = 460: k(m) = 43: rho(m) = 7.85: A(m) = “ksteel”'J/kg C, W/m K, gm/cc”

m = 4: cp(m) = 1670: k(m) = 0.162: rho(m) = 0.8: A(m) = “oil” 'J/kg C, W/m K, gm/cc 24.200 J/mol K

m = 5: cp(m) = 840: k(m) = 1.05: rho(m) = 2.5: A(m) = “glas low dens”'J/kg C, W/m K, gm/cc”

m = 6: cp(m) = 840: k(m) = 1.05: rho(m) = 3.3: A(m) = “glas med dens”' J/kg C, W/m K, gm/cc”

m = 7: cp(m) = 840: k(m) = 1.05: rho(m) = 6.2: A(m) = “glas high densi” 'J/kg C, W/m K, gm/cc

Table 1. Dimensions of type A-2 glass window components.

Item	Identifier	Density	Dimensions
A	RS253G/25	2.53	2 in. × 43 in. × 64 in.
B	RS253G/25	2.53	8-7/8 in. × 34 in. × 54 in.
C	8459	3.3	3 in. × 24 in. × 40 in.
D	8459*	3.3	8 in. × 24 in. × 40 in.
E	HI–D	6.2	6 in. × 24 in. × 40 in.
F	HI–D	6.2	6 in. × 24 in. × 40 in.
G	RS253	2.53	3/4 in. × 31-1/2 in. × 46-3/4 in.

	In		Width (in)	0.75	0.50	6.00	0.25	6.00	0.25	8.00	0.25	3.00	11.625	8.88	0.50	2.00	Q
	cre		Increments	5	2	5	2	5	2	5	2	5	5	10	2	5	
	mer	Length		g	oil	f	oil	e	oil	d	oil	c	oil	b	arg	a	
1		(inches)		1.91	3.18	18.42	19.05	34.29	34.93	55.25	55.88	63.50	93.03	115.57	116.84	121.92	cm
6	5	12		Conc		Conc		Conc		Conc		Conc	Conc	Conc		Conc	30.48
8	2	5		Conc		Conc		Conc		Conc		Conc	Conc	St	St	St	43.18
10	2	4.5		Conc		Conc		Conc		Conc		Conc	St	St	Arg	A	54.61
12	2	1.25		St		Conc		Conc		Conc		Conc	St	B	Arg	A	57.79
14	2	3.75	Corridor	G	Oil	St	Oil	St	Oil	St	Oil	St	Oil	B	Arg	A	67.31
22	8	24	air	G	Oil	F	Oil	E	Oil	D	Oil	C	Oil	B	Arg	A	128.27
24	2	3.75	htcoeff	G	Oil	St	Oil	St	Oil	St	Oil	St	Oil	B	Arg	A	137.80
26	2	1.25		St		Conc		Conc		Conc		Conc	St	B	Arg	A	140.97
28	2	4.5		Conc		Conc		Conc		Conc		Conc	St	St	Arg	A	152.40
30	2	5		Conc		Conc		Conc		Conc		Conc	Conc	St	St	St	165.10
35	5	12		Conc		Conc		Conc		Conc		Conc	Conc	Conc		Conc	195.58
Sum	34		1	6	8	13	15	20	22	27	29	34	39	49	51	56	

Figure 3. Input geometry of the window assembly.

1	Argonne		1	2	3	4	5	6	7	8	9	10	11	12	13	
2	concrete	1	2	2	2	2	2	2	2	2	2	2	2	2	2	12
3	steel	2	2	2	2	2	2	2	2	2	2	2	3	3	3	5
4	Mineral c	3	2	2	2	2	2	2	2	2	2	3	3	1	5	4.5
5	glas 2.5	4	3	2	2	2	2	2	2	2	2	3	5	1	5	1.3
6	glas 3.3	5	5	4	3	4	3	4	3	4	3	4	5	1	5	3.8
7	glas 6.2	6	5	4	7	4	7	4	6	4	6	4	5	1	5	24
		7	5	4	3	4	3	4	3	4	3	4	5	1	5	3.8
		8	3	2	2	2	2	2	2	2	2	3	5	1	5	1.3
		9	2	2	2	2	2	2	2	2	2	3	3	1	5	4.5
		10	2	2	2	2	2	2	2	2	2	2	3	3	3	5
		11	2	2	2	2	2	2	2	2	2	2	2	2	2	12

Figure 4. Material specifications.

Properties of glass are given in [7]. Normal glass (referred to here as low density) specific heat and thermal conductivity were used for medium density and high density glass. As will be seen, since the heat from combustion did not have enough time to reach the medium and high density glass before combustion was completed, this assumption had no effect on the conclusions reached. Mineral oil properties are from [8]. Properties of PVC are taken from the Wikipedia web page [9].

3. Results

A summary of the physical situations and results is included in **Table 2** with detailed results following.

1) *Base case run with* 12 *kg dendrites burning* (*HFEFWindow*1.*xlsm*).

The base case is a fire of 12 kg of uranium dendrites. The heat from one quarter or 3 kg is assumed to be applied directly to the entire Pane A. This amounts to 7.26 kW applied to the window. The area of the window is

$$\text{Pane A} = 43 * 64 * 2.54 * 2.54 = 17{,}754.8 \text{ cm}^2.$$

The heat flux per unit area is

$$\frac{Q}{A} = \frac{150 \text{ kW}}{62.18 \text{ kg}} * 3 \text{ kg} * \frac{1000 \text{ W}}{1 \text{ kW}} * \frac{1}{17754.8 \text{ cm}^2} * \frac{100 \text{ cm}}{\text{m}}$$

$$\frac{Q}{A} = \frac{40.35 \text{W}}{\text{cm m}}$$

The temperature distribution in Pane A (the heavy lined area), the steel and concrete adjacent to it, the argon layer between Pane A and B, and the surface temperature of Pane B (heavy lined open box) is shown in **Table 3**. The top row is the distance from the corridor in cm, the next to the last column is the material in the last pane, and the last column is the surface heat flux incident on the window. All empty boxes in that column are considered insulated and after the completion of combustion, the window is also insulated. This temperature is at the maximum temperature just as the last of the metal uranium has reacted to oxide. The initial temperature of the window is specified to be 35˚C. The temperature increase occurs in Pane A and very little in Pane B.

The temperature at the center of Pane A on the cell side of the glass versus time in minutes is shown in **Figure 5**. The above spatial distribution corresponds to the completion of combustion and maximum temperature. The temperature decreases sharply at the end of combustion but then drops slowly after combustion because the cell side of the glass is assumed insulated and all heat loss must eventually occur out of the corridor side of the window.

Figure 6 emphasizes the fact that the temperature increase occurs in the argon between Pane A and B and Pane A.

Boundary locations between the materials are at the center of the window.

There is a small temperature rise in the cell side of Pane B.

An expanded view of the temperatures in Panes A and Bare shown in **Figure 7**.

Table 2. List of cases investigated and results.

1. Base case run with 12 kg dendrites burning (HFEFWindow1.xlsm). The heat source is 3 kg ∗ 150 kW/62.81 kg = 7.26 kW applied on the whole area. Pane A does not crack.

2. Base case with one half power for twice as long. (HFEFWindow2.xlsm). Decreased temperatures. Pane A does not crack.

3. Full power for twice as long (HFEFWindow3.xlsm). Increased temperatures in Pane A. Pane B small heat up. Stress not significantly increased in Pane A over base case. Stress in Pane B.

4. Concentrated heat flux cosine function heating (HFEFWindow4.xlsm). Center of heat flux centered on window. Stress is high enough that Pane A could crack. If Pane A stays in place, Pane B small heat up and small stress and will not crack.

5. Pane A disintegrated. Heat radiated directly to Pane B (HFEFWindow5.xlsm). Maximum was centered on center of window. Pane A and argon layer removed. Pane B could crack. If Pane A is open or removed, exposed material should be limited.

6. Maximum heat flux centered in location of the seal with Pane A removed (HFEFWindow6.xlsm). The seal would not degrade. Pane B could crack. If Pane A is open or removed, exposed material should be limited.

7. Maximum heat flux centered in location of the seal. Pane A in place (HFEFWindow7.xlsm). Pane A could crack. Pane B does not crack.

8. Pane A is assumed to break. Remainder of the heat is applied to Pane B (HFEFWindow8.xlsm). Pane A is assumed to break 1000 psi below the stress limit and is instantaneously removed. Remainder of heat is applied to Pane B. Pane B does not reach the stress limit and does not crack.

Table 3. Temperature distribution at the end of combustion.

115.57	116.205	116.84	117.856	118.872	119.888	120.904	121.92		
35.00003	35.00004	35.00004	35.00004	35.00005	35.00005	35.00005	35.00005		
35.00004	35.00004	35.00004	35.00004	35.00005	35.00005	35.00005	35.00005		
35.00066	35.00071	35.00075	35.00082	35.00088	35.00092	35.00094	35.00094	Conc	
35.01075	35.01149	35.01219	35.01332	35.01426	35.01494	35.01529	35.01529		
35.14047	35.14988	35.15903	35.17366	35.18599	35.19507	35.19995	35.19995		
36.3815	36.4721	36.5667	36.71808	36.84632	36.94585	37.00484	37.00484		
36.41457	36.50733	36.60421	36.75923	36.89057	36.9925	37.05293	37.05293	St	
35.97127	36.52058	36.63131	38.16231	38.54203	39.13358	39.94224	40.97364		40.35226
35.57231	62.16153	89.05606	89.8757	99.41035	118.0476	146.434	185.4796	glass A	40.35226
35.75516	65.9619	94.78178	95.6601	105.688	125.0912	154.162	193.2076		40.35226
37.83518	67.01755	96.37226	97.26688	107.4318	127.0477	156.3086	195.3543	glass A	40.35226
37.89629	67.27651	96.80122	97.70102	107.8886	127.5356	156.8197	195.8653		40.35226
38.07963	68.05339	98.0881	99.00344	109.2592	128.9991	158.3527	197.3984	glass A	40.35226
38.08543	68.08699	98.14468	99.06072	109.3185	129.0609	158.4164	197.462		40.35226
38.0947	68.14074	98.2352	99.15236	109.4134	129.1599	158.5181	197.5637		40.35226
38.09496	68.14258	98.23829	99.15549	109.4166	129.1632	158.5215	197.5671		40.35226
38.09497	68.14264	98.23838	99.15558	109.4167	129.1633	158.5216	197.5672		40.35226
38.09497	68.14264	98.23838	99.15558	109.4167	129.1633	158.5216	197.5672	glass A	40.35226
38.09497	68.14264	98.23838	99.15558	109.4167	129.1633	158.5216	197.5672		40.35226
38.09496	68.14258	98.23829	99.15549	109.4166	129.1632	158.5215	197.5671		40.35226
38.0947	68.14074	98.2352	99.15236	109.4134	129.1599	158.5181	197.5637		40.35226
38.08543	68.08699	98.14468	99.06072	109.3185	129.0609	158.4164	197.462		40.35226
38.07963	68.05339	98.0881	99.00344	109.2592	128.9991	158.3527	197.3984	glass A	40.35226
37.89629	67.27651	96.80122	97.70102	107.8886	127.5356	156.8197	195.8653		40.35226
37.83518	67.01755	96.37226	97.26688	107.4318	127.0477	156.3086	195.3543	glass A	40.35226
35.75516	65.9619	94.78178	95.6601	105.688	125.0912	154.162	193.2076		40.35226
35.57231	62.16153	89.05606	89.8757	99.41035	118.0476	146.434	185.4796	glass A	40.35226
35.97127	36.52058	36.63131	38.16231	38.54203	39.13358	39.94224	40.97364		40.35226
36.41457	36.50733	36.60421	36.75923	36.89057	36.9925	37.05293	37.05293	St	
36.3815	36.4721	36.5667	36.71808	36.84632	36.94585	37.00484	37.00484		
35.14047	35.14988	35.15903	35.17366	35.18599	35.19507	35.19995	35.19995		
35.01075	35.01149	35.01219	35.01332	35.01426	35.01494	35.01529	35.01529	Conc	
35.00066	35.00071	35.00075	35.00082	35.00088	35.00092	35.00094	35.00094		
35.00004	35.00004	35.00004	35.00004	35.00005	35.00005	35.00005	35.00005		
35.00004	35.00004	35.00004	35.00004	35.00005	35.00005	35.00005	35.00005		

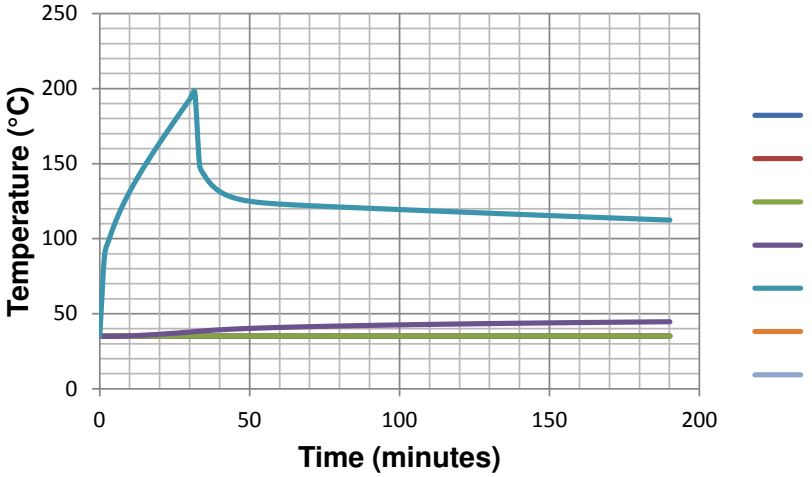

Figure 5. Temperature along the center of the glass.

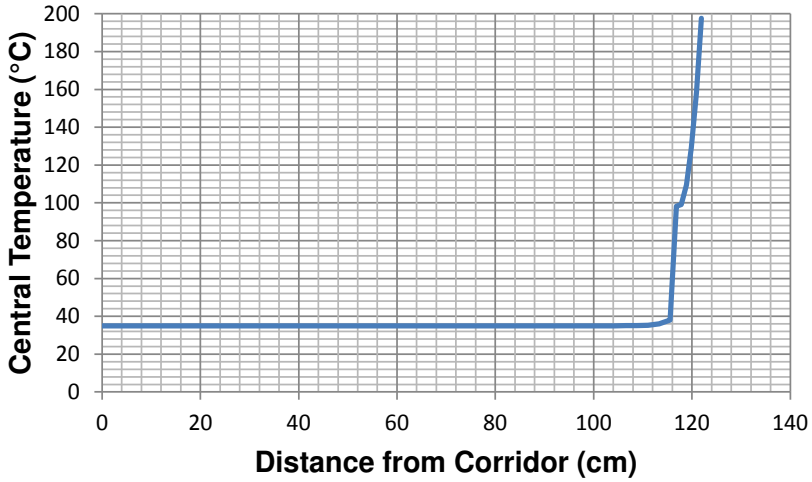

(Dimensions 93.03 cm; Pane B113.57 cm; argon116.84 cm; Pane A 121.92 cm)

Figure 6. Temperature distribution along the center of the window.

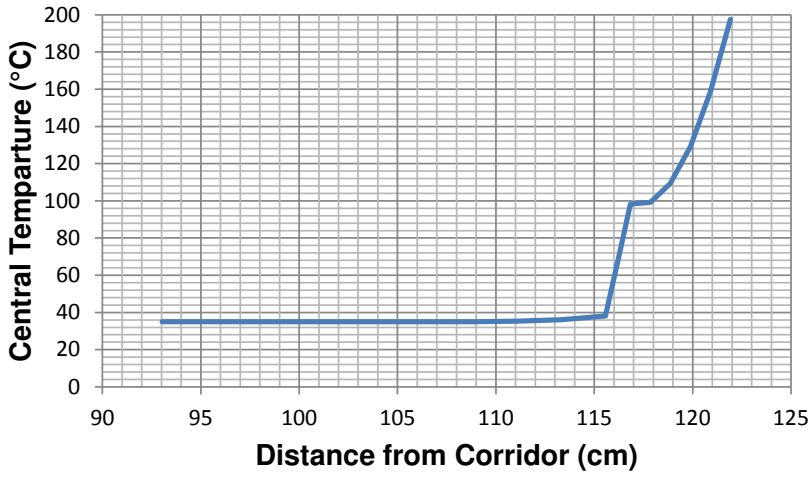

Figure 7. Temperature from corridor side of Pane B to cell side of Pane A.

The temperature distribution along the level of the window seal is shown in **Figure 8**. Just like the center temperature is almost flat in Pane B and starts to rise in the argon space, then rises in the Pane A glass. Note that the seal temperature is very low.

The calculated stress through the center of Pane A is shown in **Figure 9**.

As mentioned in the equation section, the tension stress limit for glass is listed as 40 MPa = 5714 psi. The calculated stress is less than the limit so cracking would not occur. The toughened glass limit is three to five times greater than the tension stress limit at 120 to 200 MPa. The compression limit is 1000 MPa = 142,900 psi. Compression of glass is usually not a problem and is certainly not in this situation.

2) *Base-case with one-half power for twice as long* (*HFEFWindow2.xlsm*).

To investigate combustion at a lower rate, for example, due to oxygen starvation of the reaction in a can of dendrites, a run was made with half the power for twice the time for the same total heat flux. The maximum temperature is shown **Figure 10**. The maximum temperature is lower (160˚C versus 200˚C) and the stress is about half of the base case (2000 psi versus 4000 psi).

3) *Full power for twice as long* (*HFEFWindow3.xlsm*).

The base case was rerun assuming combustion continued for twice as long. The maximum temperature time history is shown in **Figure 11**. As expected, the temperature continues to rise until the end of combustion and reaches almost 290˚C, which is 90˚C higher than the base case.

The stress in Pane A is shown in **Figure 12**.

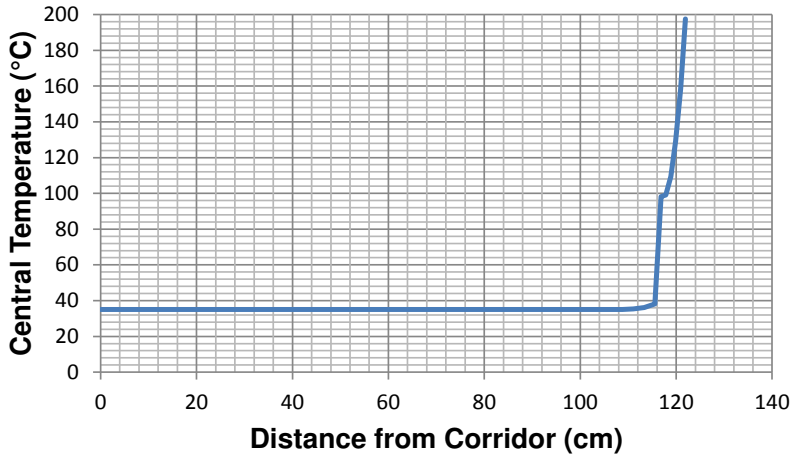

sealseal ← location of seal
Dimensions 93.03 cm Pane B 113.57 cm argon 116.84 cm Pane A 121.92 cm

Figure 8. Temperature along the level of the seal.

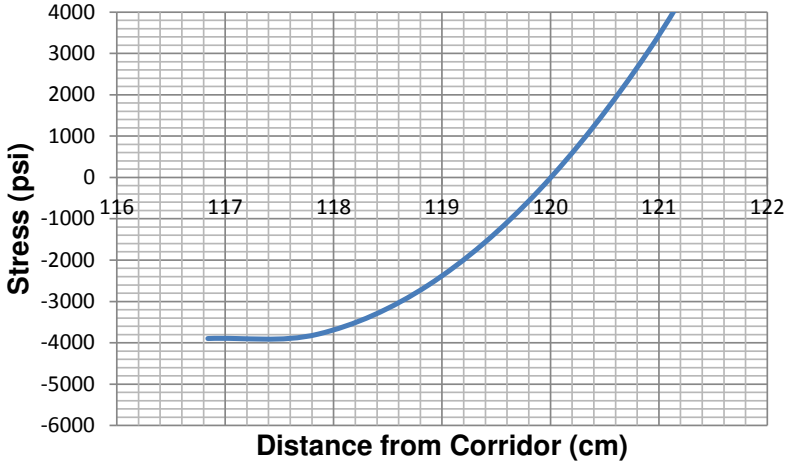

Figure 9. Stress levels in Pane A (Tension is negative and compression is positive.).

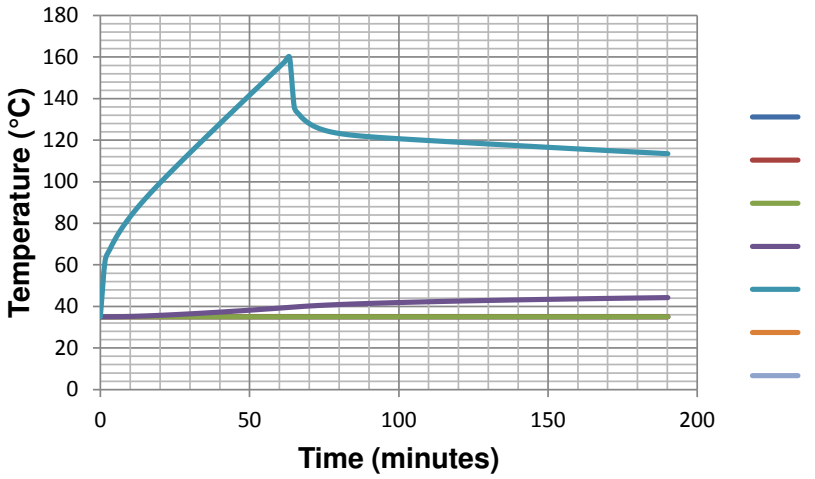

Figure 10. Investigation of effect of extending of the combustion time with the same total heat flux.

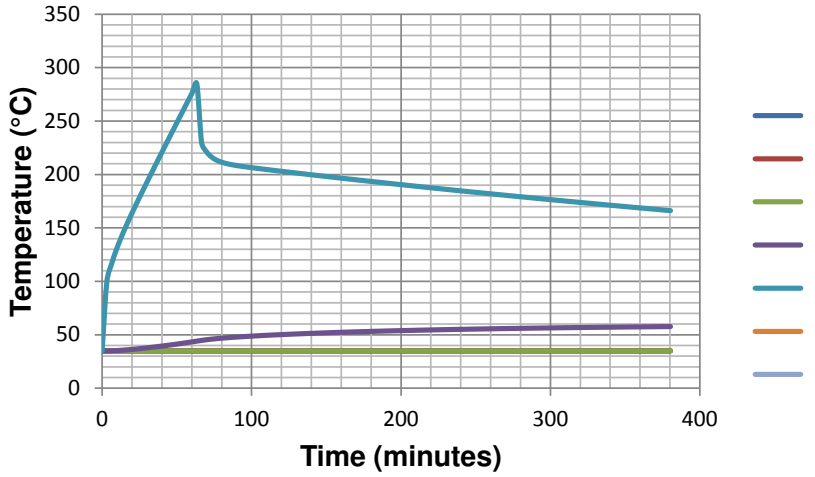

Figure 11. Investigation of the effect of doubling the total heat flux to the windows.

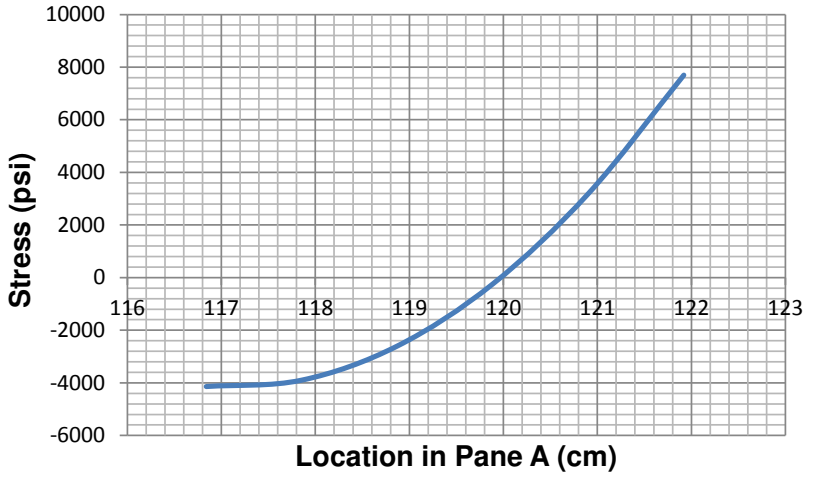

Figure 12. Stress in Pane A at the end of combustion.

The stress result is not much different than the shorter base case run. This is due to the whole temperature profile increasing in Pane A. That is, the shape is almost constant even though it is increasing and the stress depends on the temperature profile and not the absolute temperature. The temperature in Pane B heats up more than the base case, but the stress is still low (less than 200 psi).

These results imply that the maximum stress depends upon the rate of heat addition and not the total heat.

4) *Concentrated heat flux cosine function heating* (*HFEFWindow*4.*xlsm*).

The case with the same heat rate applied to the window but distributed with a cosine function was studied to determine the effect of the thermal radiation being concentrated as a result of view factors (e.g., if all the burning dendrites are in a canister).The same total heat flux was assumed to heat the window. The distribution shown in **Figure 13** was assumed with the maximum being at the center of the window and the end from zero at the edge of the window.

The temperature at the center of the window (shown in **Figure 14**) is higher by 100˚C than the base case.

The stress along the centerline of Pane A is shown in **Figure 15**. The Pane Astress exceeds the tensile stress limit for a short time making it possible that this pane will crack.

This glass, even though cracked, could stay in place because of its thickness and the lack of a pressure difference between. The case where it completely falls out is investigated in a later calculation. If it stays in place, Pane B only heats up to 50˚C. The stress in Pane B in this case is shown in **Figure 16** and is seen to be far below the failure limit.

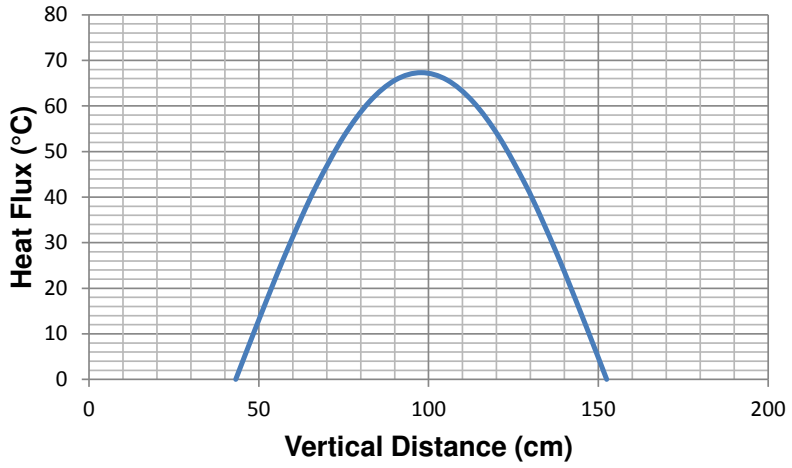

Figure 13. Cosine distribution of heat flux.

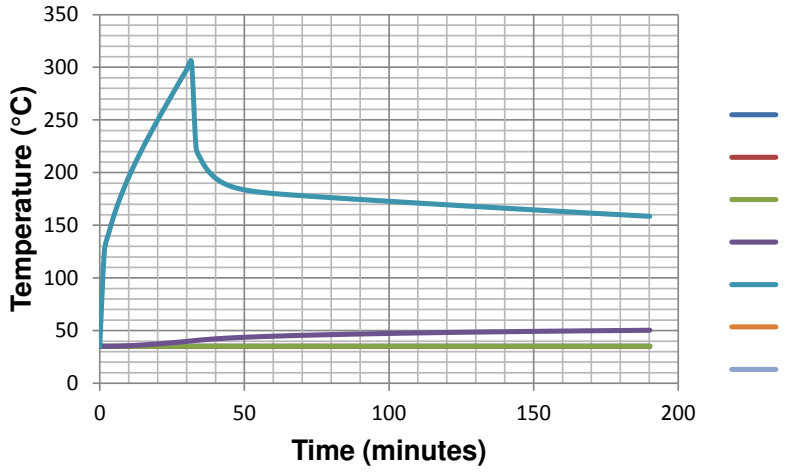

Figure 14. Maximum temperature with cosine heat flux distribution.

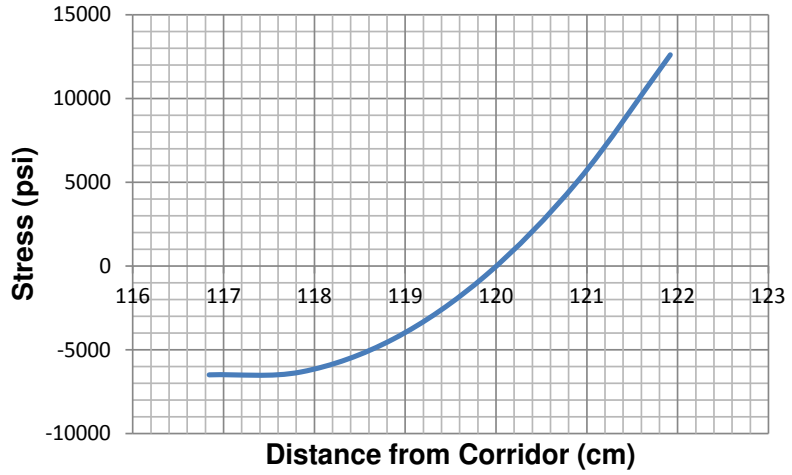

Figure 15. Stress distribution in Pane A for the cosine distribution.

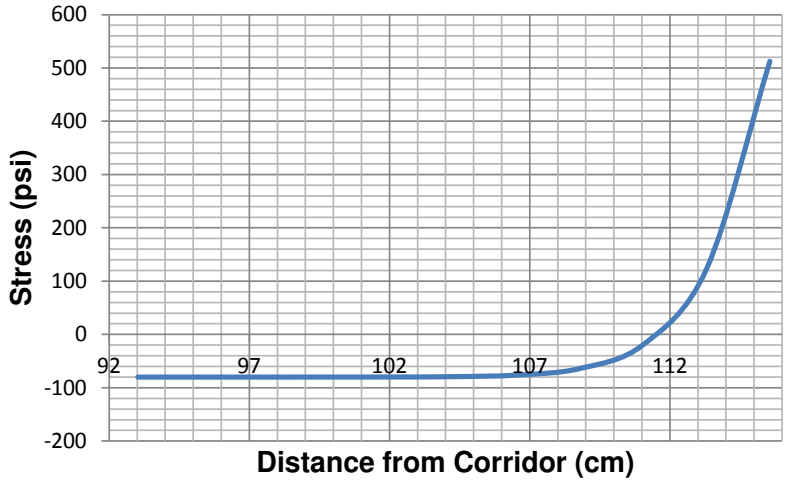

Figure 16. Stress in Pane B for the cosine distribution.

5) *Layer A disintegrated allowing the heat to radiate directly to Pane B* (*HFEFWindow5.xlsm*).

In order to assess the maximum possible danger to the HFEF window, the loss of Pane A was investigated. An analysis was conducted where Pane A was assumed disintegrated and removed. Heat radiated directly to Pane B. A cosine distribution of heat flux was centered on the window. The temperature distribution (shown in **Figure 17**) reached 340˚C on the cell side of the Pane B.

Figure 18 shows the stress limit within the highest stress plane (through the center of Pane B) and exceeded the stress limit for almost 10 cm so it could crack.

The transient stress at the highest stress location (on the corridor side of Pane B) is shown in **Figure 19**. The stress exceeds the tensile stress limit for half the depth of Pane A only for a few minutes but it is possible that this pane may crack.

Item 8 analyzes the outcome of Pane A disintegrating and exposing Pane B during the transient. The results of this analysis indicate that the amount of exposed material should be reduced during operation if the Pane A is open or removed for programmatic reasons.

6) *Maximum heat flux centeredon the seal with Pane A removed* (*HFEFWindow6.xlsm*).

The cosine heat flux was applied with the maximum flux centered on the one side of the window seal with Pane A assumed to be open or removed. The transient temperature in the seal is shown in **Figure 20**.

Figure 21 shows the spatial profile at the seal horizontal location and the temperature on both sides of Pane B. The temperatures are low enough that no seal degradation is expected.

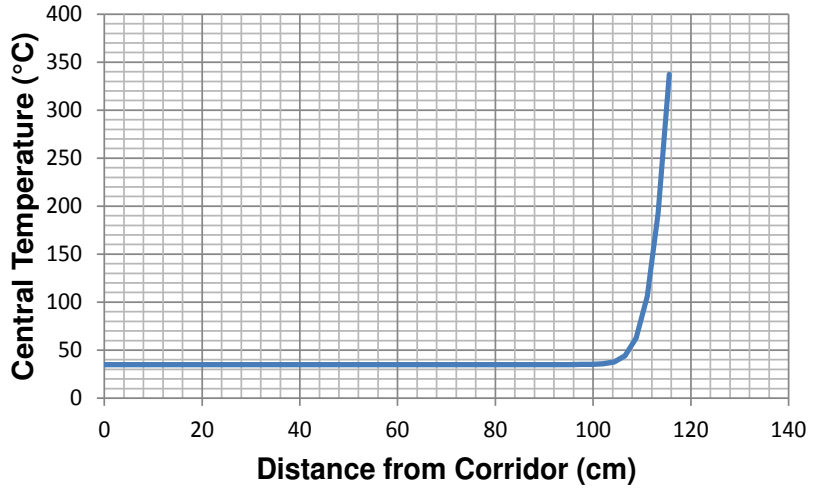

Figure 17. Temperature distribution with Pane A removed.

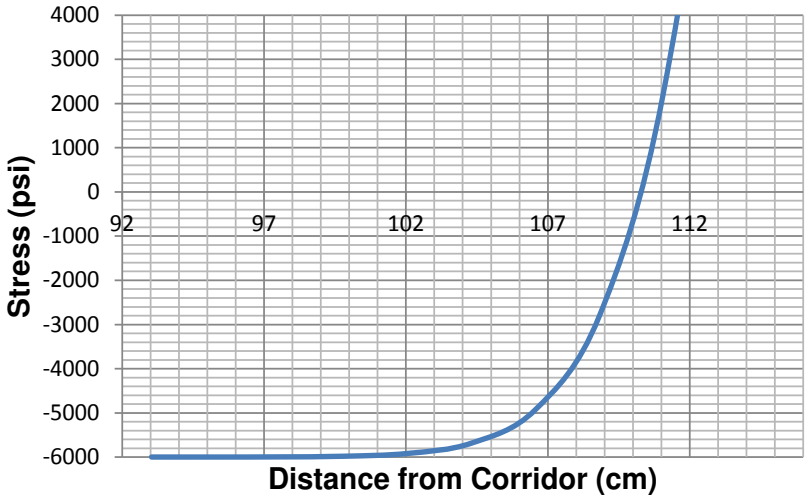

Figure 18. Stress in Pane B for the cosine distribution and with Pane A removed.

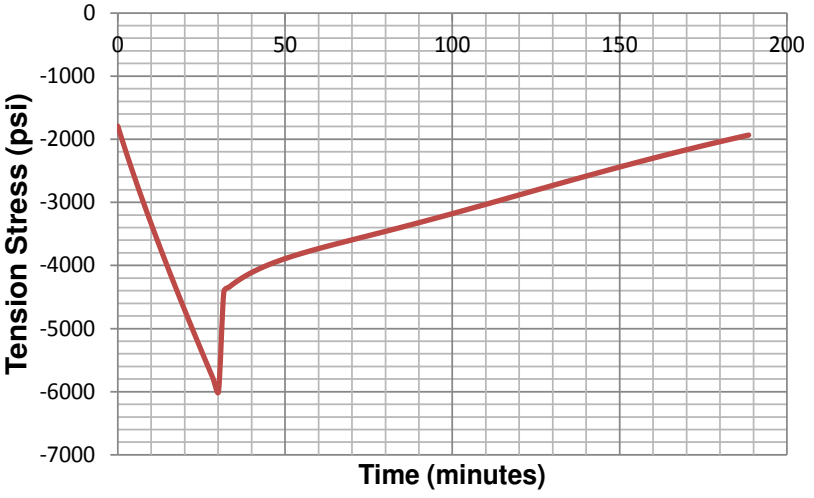

Figure 19. Transient stress on corridor side of Pane B.

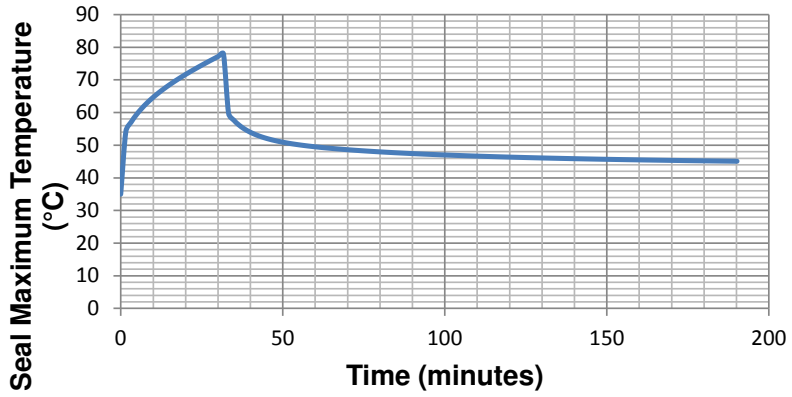

Figure 20. Transient seal temperature with Pane A removed.

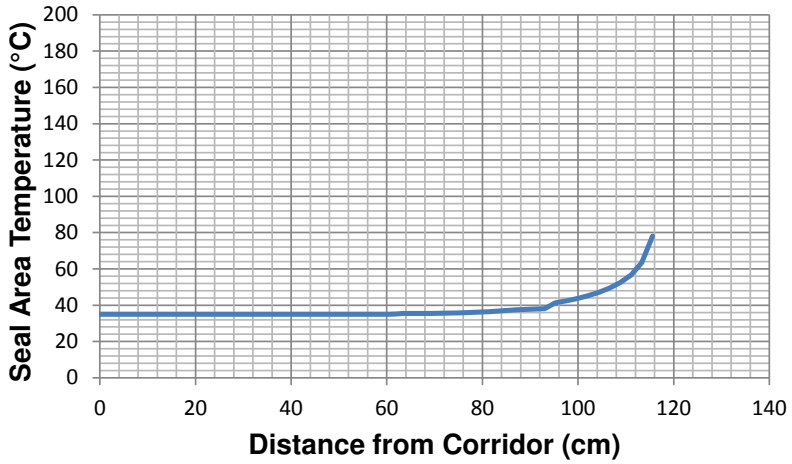

Figure 21. Temperature through seal area.

The stress through the seal area is shown in **Figure 22**. The stress (a few inches in) is a bit higher (<5200 psi) but lower throughout Pane B. The stress is not high enough to cause any damage to Pane B.

The oil temperature (**Figure 23**) increase is the highest in this scenario since the heat flux is centered near the edge of the glass. Heat can be conducted to the oil through the concrete better than though the glass. The maximum temperature occurs at the edge of the tank and is only 0.4 C above the starting temperature. The average temperature over the whole tank is only 35.03 C. The volumetric expansion coefficient [8] (Ref. Godfrey, 1995) of mineral oil is 6.4×10^{-4} C. The overall temperature increase of 0.03 C results in a volume increase of 0.0014 gallons over the original 75 gallons. Therefore the expansion of the oil is quite small and not of concern.

Also, the C pane (3 inches) is much thinner than the B pane (8.75 inches) so that it should crack before the B pane. This has in fact happened when the oil was pressurized with a positive displacement pump. In this case, any leaking oil would go toward the corridor instead of the cell.

7) *Maximum heat flux centered on the seal with Pane A in place.* (*HFEFWindow*7.*xlsm*)

The temperature at the seal horizontal location is shown in **Figure 24**. The seal temperature remains less than 50˚C. No degradation of the seal is expected.

The stress profile in Pane A at the directly in front of the seal is shown in **Figure 25**. This is the maximum stress in Pane A. Pane A may crack because the stress levels exceed the stress limit. The stress in Pane B is low (<300 psi); there is no danger of it cracking.

8) *Pane A is assumed to break. Then heat applied directly to Pane B* (*HFEFWindow*8.*xlsm*).

The stress in Pane A is assumed to cause it to crack slightly below the tensile stress limit of 5714 psi. The transient stress at the center and on the corridor side of Pane A is shown in **Figure 26**. It is seen that the stress increases quite quickly but approaches a constant near the end of the transient. At 12.67 minutes and a stress of

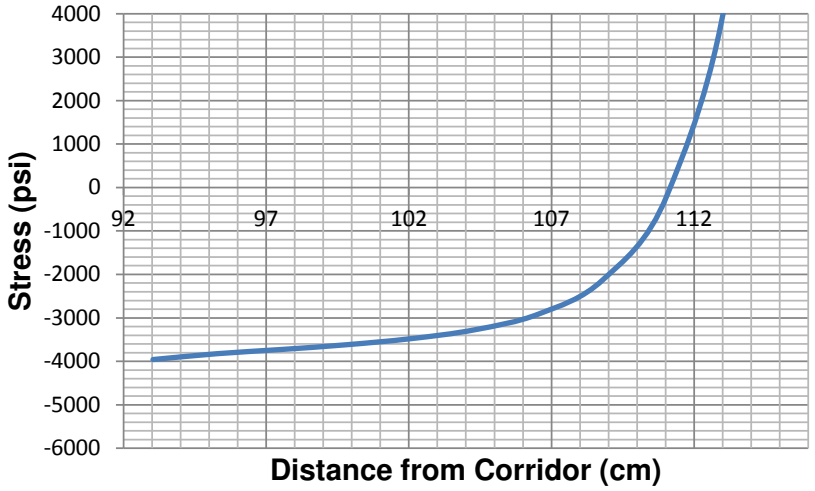

Figure 22. Stress throughout seal area.

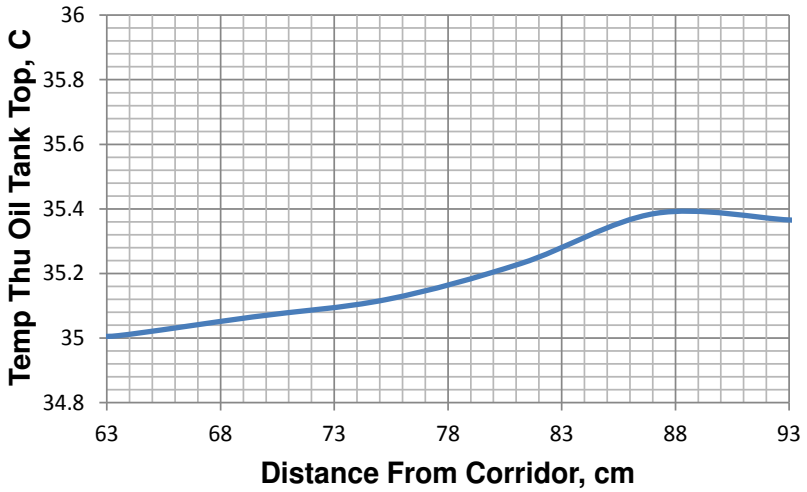

Figure 23. Oil temperature.

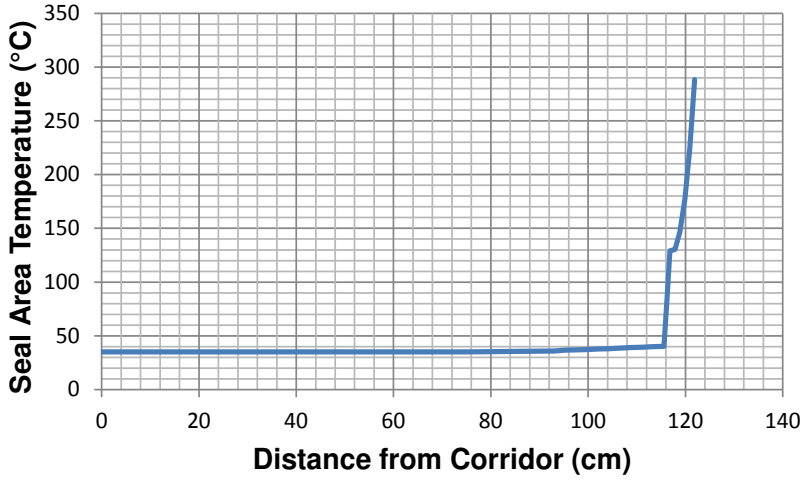

Figure 24. Temperature profile through the seal with Pane A (in place).

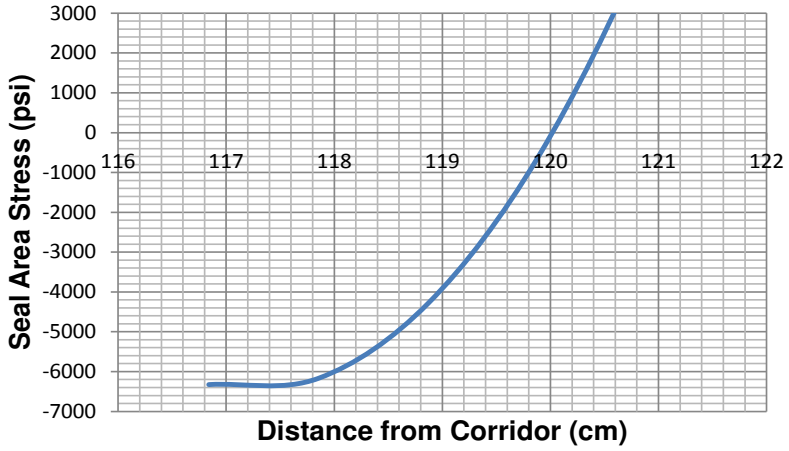

Figure 25. Stress in Pane A at seal area level.

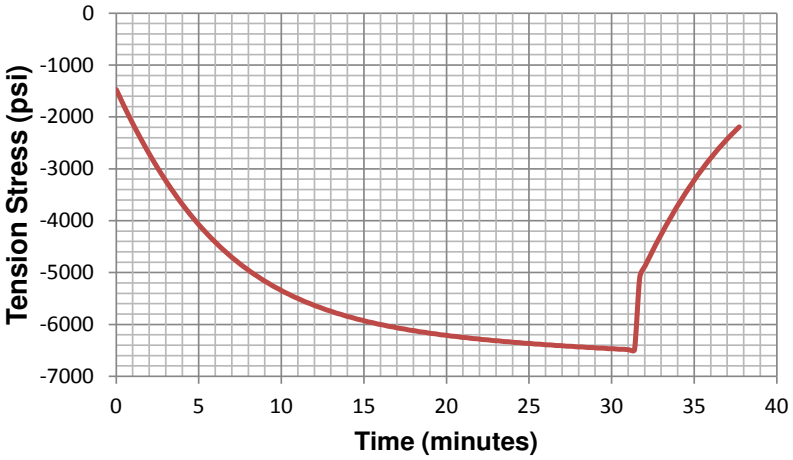

Figure 26. Stress in Pane A assumed to break at 5600 psi.

5600 psi, even though Pane A is 2 inches thick, it is assumed to rupture and completely disappear. Then all the heat from the fire is applied directly to Pane B.

Figure 27 shows the resulting transient stress at the center and on corridor side of Pane B.

The results in **Figure 27** show the stress does not reach the tensile limit and only reaches 4400 psi.

As an additional conservatism, a case was run assuming that the tensile limit is actually 500 psi below the stated tensile limit. Pane A is assumed to fracture at 9.02 minutes at a stress of 5200 psi.

The stress in the center corridor side of Pane B when all the combustion heat is applied directly to Pane B at 9.02 minutes is shown in **Figure 28**. The stress is larger than the previous case but still remains below assumed lower stress limit of 5200 psi.

4. Discussion of Results

The heat flux to the exposed window is quite high for the amount of metal assumed to be burning. It is assumed that all the material is dendrites (releases the highest heat flux of any material handled). It is more likely made-up of a mixture of lower-burning and high-burning rates. Also, it is unlikely that 12 kg will be exposed. One-fourth of the heat released is assumed to reach the window by thermal radiation. Due to the geometry, it is likely to be less. Also, convective losses to the cell environment are neglected. That is, if the metal fire itself were modeled in detail, the heat flux to the windows from 12 kg of burning dendrites would be less than assumed here. Also, the material will likely be distributed between two windows rather than concentrated in front of one window.

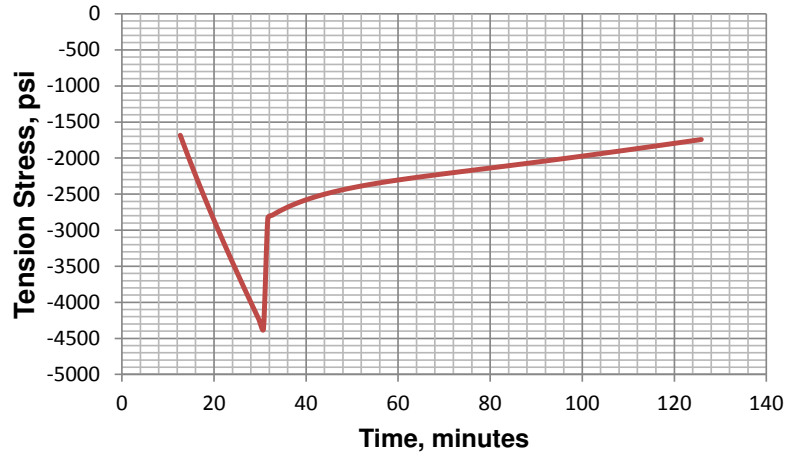

Figure 27. Stress at the mid plane on the corridor side of Pane B.

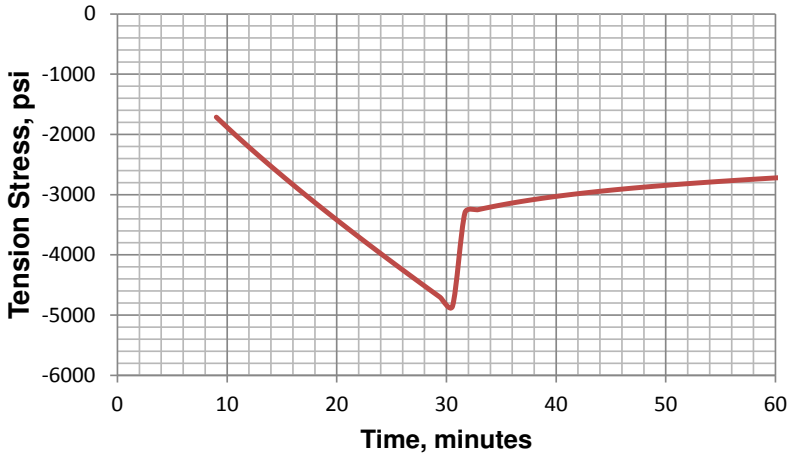

Figure 28. Midplane stress on the corridor side of Pane B assuming Pane A fractures at 5200 psi.

Most of the runs conducted were started with protective Pane A in place. When this pane is in place, the temperature rise barely reaches Pane B so there is no danger of Pane B breaking which is the window which forms a wall of the oil reservoir.

If Pane A completely disintegrates, it would expose Pane B to the heat flux at some point into the transient; however, since it is 2 inches thick, it is likely that it could remain in place even if cracked. The possible cracking of Pane B is significant because it is the barrier for the flammable mineral oil. None of the cases investigated indicate that Pane B will crack unless Pane A is removed or non-existent for the entire fire. If Pane A is missing, the amount of exposed material should be reduced.

In order to investigate the breaking of Pane A conservatively, it was assumed to be missing completely and the heat was applied directly to Pane B at the start of combustion. This also investigates the case if the fire happens if Pane A is open for cleaning. Pane B could crack when the heat is directly applied for the entire combustion event.

The heat flux was applied on the center of the seal. The seal did not heat up to 140˚C where it could degrade. This is true whether or not Pane A is in place.PVC starts to decompose when the temperature reaches 140˚C with melting temperature starting around 160˚C.

A final case was investigated where Pane A was assumed to instantly disintegrate at the stress limit of 5700 psi and then the remaining heat was directly applied to Pane B. The thermal stress in Pane B did not exceed 4400 psi. A further case was run with Pane A assumed to disintegrate 500 psi below the stress limit at 5200 psi. The stress in Pane B remained below the stress limit reaching only 4900 psi.

5. Conclusions

The results indicate that in the worst case from a fire of 12 kg of dendrites during normal operation, Pane A could break and then expose Pane B to the remaining heat from the fire. Even in this case Pane B will not crack. This is the most stressful burning rate of the materials being processed. In the non-normal operation case where removable Pane A has been removed for repair or cleaning, Pane B would crack but would not break away and so probably would not allow much if any oil to leak from the window. In most operations, the amount of material exposed will be less than 12 kg and have lower heat-release rates so that Pane A will not break.

Since Pane B will not break, mineral oil will not be released into the cell so it will not ignite and add heat to the cell A previous study showed that combustion of a much larger amount of dendrites, 62.81 kg, only raises the cell atmosphere temperature by 35˚C. This temperature level is not high enough to cause the release of volatiles from other materials; therefore, no flashover of fire in the cell is possible from the smaller 12 kg heat source considered in this study.

The analysis presented here assumed that all the heat reaching the window was transmitted in the window by conduction but in reality, some would be transmitted through the glass to the surrounding corridor. The assumption of no transmission through the window increases the temperature gradients in the glass panes which increases the thermal stress. Thus the cases which showed pane A cracking and breaking away, in reality probably would not occur because the heat reducing effect of the transmission of radiant energy through the window was not taken into account.

Acknowledgements

This work is supported by the US Department of Energy, Office of Nuclear Energy, under DOE Idaho Operations Office Contract DE-AC07-05ID14517. Accordingly, the US Government retains a nonexclusive, royalty-free license to publish or reproduce the published form of this contribution, or allow others to do so, for US Government purposes.

Disclaimer

This information was prepared as an account of work sponsored by an agency of the US Government. Neither the US Government nor any agency thereof, nor any of their employees, makes any warranty, expressed or implied, or assumes any legal liability or responsibility for the accuracy, completeness, or usefulness of any information, apparatus product, or process disclosed, or represents that is use would not infringe privately owned rights. References herein to any specific commercial product, process, or service by trade name, trademark, manufacturer, or otherwise, do not necessarily constitute or imply its endorsement, recommendation, or favoring by the US Government or any agency thereof. The views and opinions of authors expressed herein do not necessarily state or reflect those of the US Government or any agency thereof.

Conflict of Interests

The authors declare that there is no conflict of interests regarding the publication of this paper.

References

[1] Solbrig, C.W. (2009) Mathematical Model of the Hot Fuel Examination Facility Main Cell Response to Breaches. ECAR-534, Idaho National Laboratory.

[2] SAR 405, Safety Analysis Report for the Hot Fuel Examination Facility, Enclosure 2, 2014.

[3] Timoshenko, S. and Goodier, J.N. (1970) Theory of Elasticity. 3rd Edition, McGraw-Hill, New York.

[4] Solbrig, C.W. and Bateman, K.J. (2010) Modeling Solidification-Induced Stress in Ceramic Waste Forms Containing Nuclear Wastes. *Nuclear Technology*, **172**, 189-203.

[5] (Gobain) Saint Gobain Glass UK, Glass Mechanical Properties. http://uk.saint-gobain-glass.com/trade-customers/physical-properties

[6] (Lehman) The Mechanical Properties of Glass, Glass Engineering 150:312 Professor Richard Lehman, Department of Ceramics and Materials Engineering, Rutgers University, New Brunswick. http://glassproperties.com/references/MechPropHandouts.pdf

[7] Shand, E.B. (1958) Glass Engineering Handbook. 2nd Edition, McGraw-Hill, New York.

[8] Godfrey, D. and Herguth, W.R. (1955) Physical and Chemical Properties of Industrial Mineral Oils Affecting Lubrication, Part 2. *Journal of the Society of Tribologists and Lubrication Engineers*.

[9] (PVC Web Page) Polyvinyl Chloride Thermal, Melting and Decomposition Properties Taken from Web Page. http://en.wikipedia.org/wiki/Polyvinyl_chloride#Physical_properties